iScience

Article

Activated PRDM1-CREBBP contributes to preeclampsia by regulating apoptosis and invasion of the human trophoblast cells

Graphical abstract

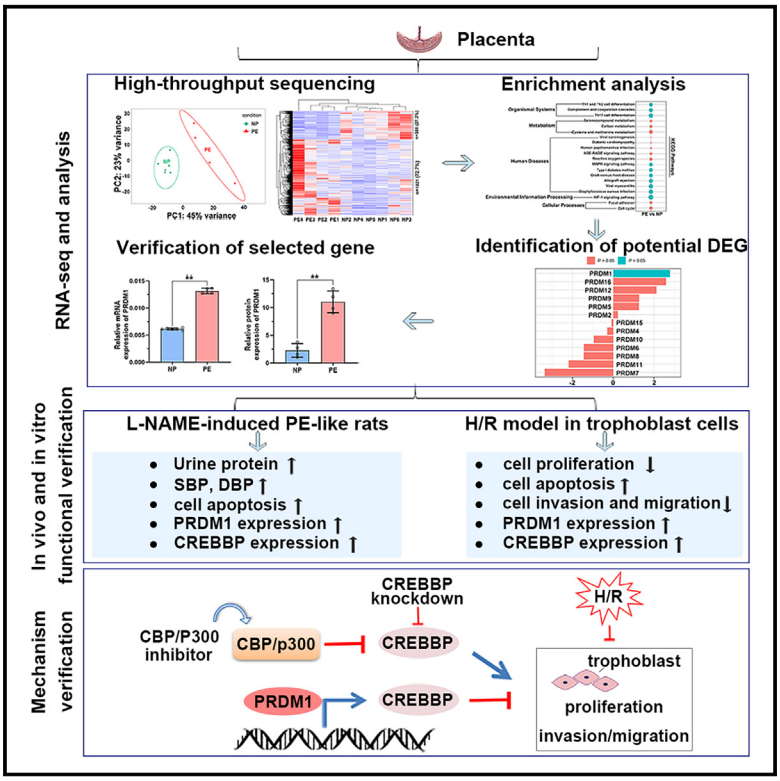

Highlights

- PRDM1 overexpressed in placenta from patients with PE and L-NAME-treated rats
- Inhibition of PRDM enhanced cell invasion and reduced apoptosis of trophoblast cells
- CREBBP was demonstrated as a direct target of PRDM1 in trophoblast cells
- PRDM1 impaired trophoblast cell function by transcriptionally upregulating CREBBP

Authors

Xuan Zhang, Lei Sun

Correspondence

sjfck189@163.com

In brief

Cardiovascular medicine; Cell biology

Zhang & Sun, 2024, iScience 27, 111484
December 20, 2024
https://doi.org/10.1016/j.isci.2024.111484

CellPress

iScience

CellPress
OPEN ACCESS

Article

Activated PRDM1-CREBBP contributes to preeclampsia by regulating apoptosis and invasion of the human trophoblast cells

Xuan Zhang[1] and Lei Sun[1,2,*]
[1]Department of Obstetrics and Gynecology, Shengjing Hospital of China Medical University, Shenyang 110004, P.R. China
[2]Lead contact
*Correspondence: sjfck189@163.com
https://doi.org/10.1016/j.isci.2024.111484

SUMMARY

Preeclampsia (PE) is a multifactorial disorder of pregnancy, characterized by new-onset gestational hypertension. High-throughput mRNA sequencing (RNA-seq) was performed to analyze the gene expression patterns in placentas from patients with early-onset PE (EOPE). PR domain zinc-finger protein 1 (PRDM1) expression increased in the chorionic villi and placental basal plate from patients with PE and nitro-/-arginine methyl ester (L-NAME)-treated rats. Inhibition of PRDM1 enhanced trophoblast/extravillous trophoblast (EVT) cell invasion/migration and reduced apoptosis under hypoxia/reoxygenation (H/R) conditions. RNA-seq data indicated that the expression of CREB-binding protein (CREBBP), a transcriptional coactivator, was upregulated in preeclamptic placentas and showed a positive correlation with that of PRDM1. Genetic and pharmacological inhibition of CREBBP exhibited anti-apoptotic and pro-invasive roles. H/R stimulation upregulated CREBBP expression and augmented the binding of PRDM1 to CREBBP's promoter. CREBBP was further validated as a direct downstream target of PRDM1. Collectively, our work reveals an involvement of the activated PRDM1-CREBBP axis in PE-associated trophoblast dysfunction.

INTRODUCTION

Preeclampsia (PE), is a multifactorial disorder of pregnancy that has clinically been defined by new-onset or worsening maternal hypertension after 20 weeks of gestation accompanied by one or more other features: maternal organ dysfunction (including liver, kidney, neurological), or hematological involvement, and/or uteroplacental dysfunction, such as fetal growth restriction (FGR) and/or abnormal Doppler ultrasound findings of uteroplacental blood flow, are leading causes of maternal mortality and morbidity, affecting about 2%–8% of pregnancies.[1–4] PE is classified as early- and late-onset types, and early-onset PE (EOPE) is widely acknowledged to have primarily a placental cause and is associated with increased risks of neonatal mortality and maternal morbidity.[5] The human placenta is a unique organ that is necessary for the development of the embryo and for pregnancy success.[6] Defective placentation is associated with the pathogenesis of EOPE and FGR.[7,8] Trophoblast cells proliferate, migrate, and invade the maternal decidua, which is crucial for placental development, spiral artery remodeling, and subsequently fetal growth.[9] Dysregulation of trophoblasts is associated with pregnancy complications including PE.[10] Two major trophoblast cell lineages have been identified during human placental development: villous trophoblasts and extravillous trophoblasts (EVTs).[11] Inadequate trophoblast invasion into the decidua causes incomplete spiral artery remodeling, which may trigger a wide variety of pathological mechanisms that are associated with the clinical manifestations of PE.[2,12] Therefore, exploring the factors that affect the process of trophoblast cellular function is of great significance for improving the understanding of the pathogenesis of EOPE.

RNA-sequencing (RNA-seq) technology is commonly used to profile the placental transcriptome.[13,14] In the present study, we performed RNA-seq of the placentas from patients with EOPE and normal pregnant women to analyze the gene signatures. PR domain zinc-finger protein 1 (PRDM1) is a transcriptional factor with a known function in regulating the terminal differentiation of B cells[15] and the generation of antitumor T cells.[16] PRDM1 has a unique PR domain with C2H2 zinc fingers that exhibits physiological function in a transcriptional manner.[17] Both transcriptional activation and deactivation effects of PRDM1 on its targets have been revealed in previous studies.[18,19] In animal studies, PRDM1 governed the terminal differentiation of endovascular trophoblast giant cells under the physiological state in the mouse placenta.[20] A previous study identified that proliferative trophoblasts expressed PRDM1 and PRDM1 was essential for the specification of spiral artery trophoblast giant cells that invade and remodel maternal blood vessels in human[21] However, whether PRDM1 plays a role in PE-associated pathological alterations of trophoblasts remains unknown.

CREB-binding protein (CREBBP/CBP) and E1A-binding protein P300 (EP300) are ubiquitously expressed transcriptional coactivators and homologous lysine acetyltransferases that govern various cellular processes.[22,23] EP300 and CBP share

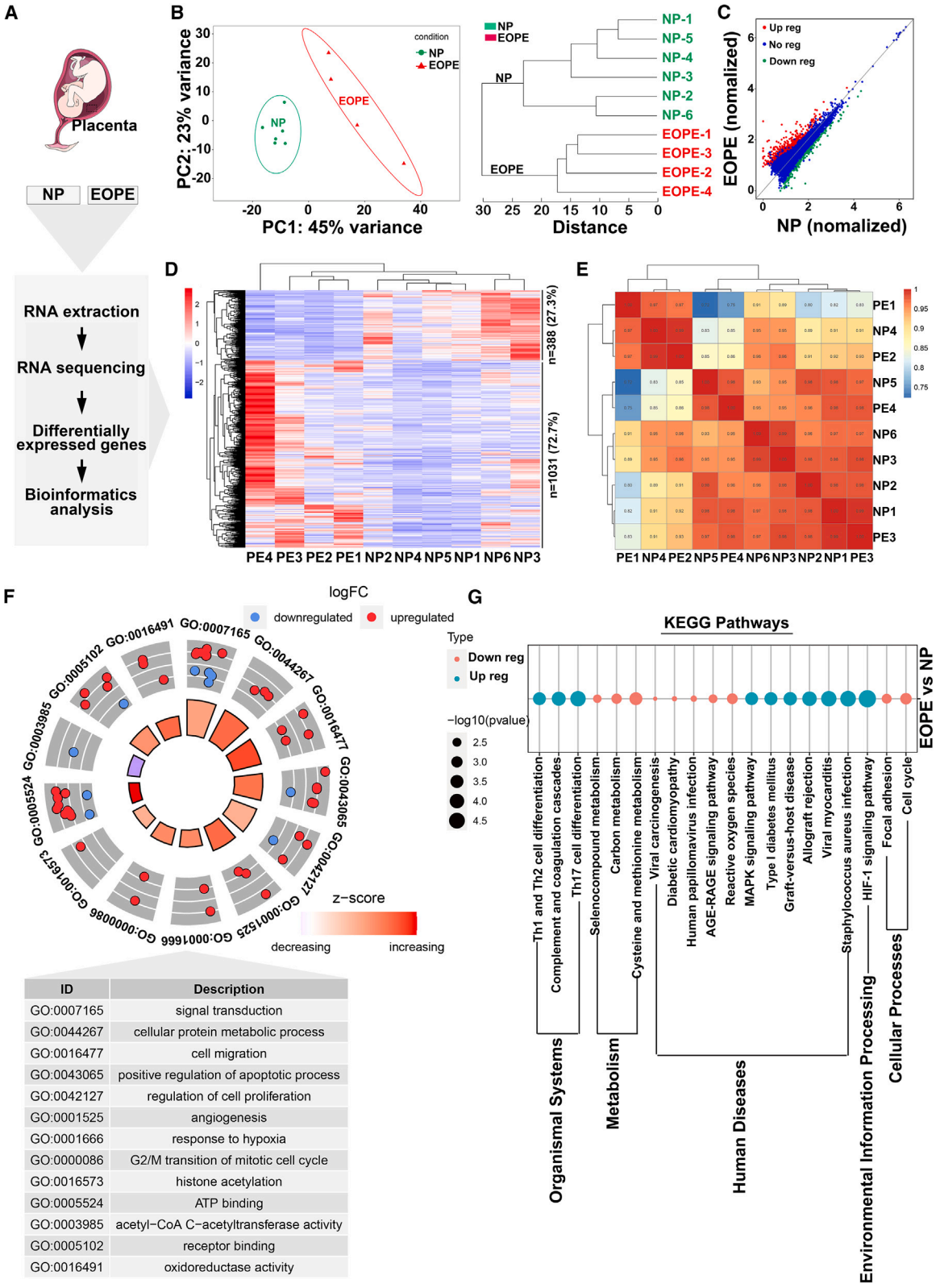

ID	Description
GO:0007165	signal transduction
GO:0044267	cellular protein metabolic process
GO:0016477	cell migration
GO:0043065	positive regulation of apoptotic process
GO:0042127	regulation of cell proliferation
GO:0001525	angiogenesis
GO:0001666	response to hypoxia
GO:0000086	G2/M transition of mitotic cell cycle
GO:0016573	histone acetylation
GO:0005524	ATP binding
GO:0003985	acetyl−CoA C−acetyltransferase activity
GO:0005102	receptor binding
GO:0016491	oxidoreductase activity

Figure 1. Gene expression analysis of EOPE and healthy placental samples

(A) Schematic representation of transcriptome from patients with early-onset PE (EOPE; *n* = 4) and the normal pregnancy (NP; *n* = 6).

(legend continued on next page)

high sequence identity in several structured regions. Sequence alignments of these two enzymes revealed a 93% homology in the bromodomain. However, the homology is substantially lower outside of these highly conserved domains. Evidence suggests that the two acetyltransferases have unique roles in cells. CREBBP is a pivotal regulator in a series of biological functions including cell proliferation, differentiation, migration, and invasion.[24,25] Recently, Sadeghi and co-workers[26] have determined a high expression of CREBBP in placental biopsies from patients with PE. In addition, CREBBP is demonstrated as a key molecule central to the placental transcriptome.[27] Interestingly, the JASPER online database (http://jaspar.genereg.net/) indicated CREBBP as a potential target of PRDM1. Therefore, we aimed to investigate the association of CREBBP to trophoblast cell invasion and to explore whether PRDM1 acts as an upstream regulator of CREBBP.

This study aimed at elucidating the underlying mechanisms of EOPE by (1) analyzing the transcriptomic alteration in placentas between patients with EOPE and healthy individuals and (2) investigating how the PRDM1-CREBBP axis affects trophoblast cellular function. PRDM1 expression in the different regions of the placenta, including the basal plate (area of EVT) and chorionic villi (the functional unit of the placenta), was detected. The expression of PRDM1 was confirmed in the placental tissues of rats of nitro-*l*-arginine methyl ester (L-NAME)-induced PE-like symptoms. Hypoxia/reoxygenation (H/R) was conducted *in vitro* to mimic the variation of oxygen in the placenta for exploration of the regulatory role of PRDM1 in trophoblast function using primary trophoblasts. Human chorionic trophoblast cell line HTR-8/SVneo was employed for further verification of the effect of PRDM1 on trophoblast cell function and the related mechanisms *in vitro*. Our hypothesis is that trophoblastic PRDM1 regulates placental development by modulating trophoblast cellular functions.

RESULTS

RNA-seq and transcriptome profiling

To determine which genes have aberrant expression in EOPE, we analyzed the mRNA expression of placentas from four patients with EOPE and six normal pregnancy (NP) via RNA-seq (Figure 1A). In the unsupervised principal component analysis (PCA) score plot, differentially expressed genes (DEGs) were separated appropriately between EOPE and NP individuals (Figure 1B, left) and segregated into tight clusters (Figure 1B, right). As shown in Figure 1C, a total of 1,031 genes (red dots) were upregulated, whereas 388 genes (green dots) were downregulated in PE placentas. RNA-seq analysis revealed 1,419 significant DEGs (Figure 1D; $|\log_2 FC| > 1$ and $p < 0.05$). By evaluating Pearson's correlation coefficient, the EOPE and control samples appeared to have relatively high correlations (Figure 1E). To explore the potential biological functions of these DEGs, we obtained the functional enrichment of these genes. Gene Ontology (GO) analysis revealed the association of DEGs with cell proliferation and migration, oxidoreductase activity, response to hypoxia, and metabolic process (Figure 1F). Furthermore, Kyoto Encyclopedia of Genes and Genomes (KEGG) analysis indicated that these DEGs were classified into five KEGG categories including metabolism process, human disease, organismal systems, environmental processes, and cellular process (Figure 1G).

Furthermore, KEGG pathway analyses revealed that the gene networks and pathways dysregulated in EOPE were associated with signal transduction pathways, such as TGF-β signaling pathway, Hippo signaling, AMPK signaling pathway, hypoxia-inducible factor 1 subunit alpha, and Wnt signaling pathway. In addition, transcriptome analysis revealed that potential genes putatively associated with PE pathogenesis (Figures S1A–S1C).

Increased expression of PRDM1 in placental trophoblasts of patients with EOPE

Among the DEGs, we noted that PRDM members might be related to EOPE development. A total of 13 PRDM members were identified (Figure 2A), including six upregulated and seven downregulated PRDMs in EOPE placental tissues. Among them, only PRDM1 showed a significant upregulation ($\log_2 FC = 2.789$; $p < 0.0001$). We further verified PRDM1 expression in placental villous tissues from four EOPE patients and six normal controls by performing real-time PCR (Figure 2B). Consistently, the mRNA expression of PRDM1 was significantly upregulated in the EOPE placentas compared with the normal placentas. We also confirmed increased PRDM1 protein expression in EOPE placenta tissues by western blot analysis (Figure 2C). To further confirm the upregulated PRDM1 in EOPE placenta, we detected PRDM1 expression based on the GSE149812 and GSE177049 datasets (Figure S1D). The results indicated that PRDM1 expression was also increased in placental tissues of patients with EOPE compared to normotensive controls ($\log_2 FC = 2.041$; p value = 0.003) and ($\log_2 FC = 0.973$; p value = 0.023), respectively.

In addition, to further identify immunolocalization and compare PRDM1 levels, human placental villous tissues and basal plates of the placenta were stained via immunohistochemistry assay. PRDM1 staining was seen in the syncytiotrophoblasts (STBs) of the chorionic villi. CK7 was utilized as a marker for trophoblast cells.[28] We then performed immunofluorescence double staining with PRDM1 and CK7 in clinical placental samples to detect PRDM1 expression. Our data demonstrated that PRDM1 was highly expressed in the placenta of patients with EOPE, prominently localized in STBs as depicted in Figure 2E. HLA-G is exclusively expressed in the EVT[29]; we used it as a marker for the EVT in the placental bed. Strong HLA-G staining was observed in the plasma membrane of all EVTs (Figure 2F). Samples that contain basal plate regions further demonstrated the upregulation of PRDM1 in invasive EVTs. Collectively, PRDM1 expression

(B) PCA revealed that NP samples clustered separately from EOPE ones (left); dendrogram of hierarchical clustering analysis from EOPE and NP groups (right).
(C) The scatterplot of all the DEGs; the upregulated genes (Up reg) were denoted in red, and the downregulated genes (Down reg) were denoted in green. Not significantly changed genes (No reg) were denoted in blue.
(D) Hierarchical clustering; 1,031 genes were upregulated and 388 genes were downregulated.
(E) Heatmap of inter-sample Pearson's correlation between PE and healthy placenta samples.
(F and G) GO and KEGG functional classification of DEGs.

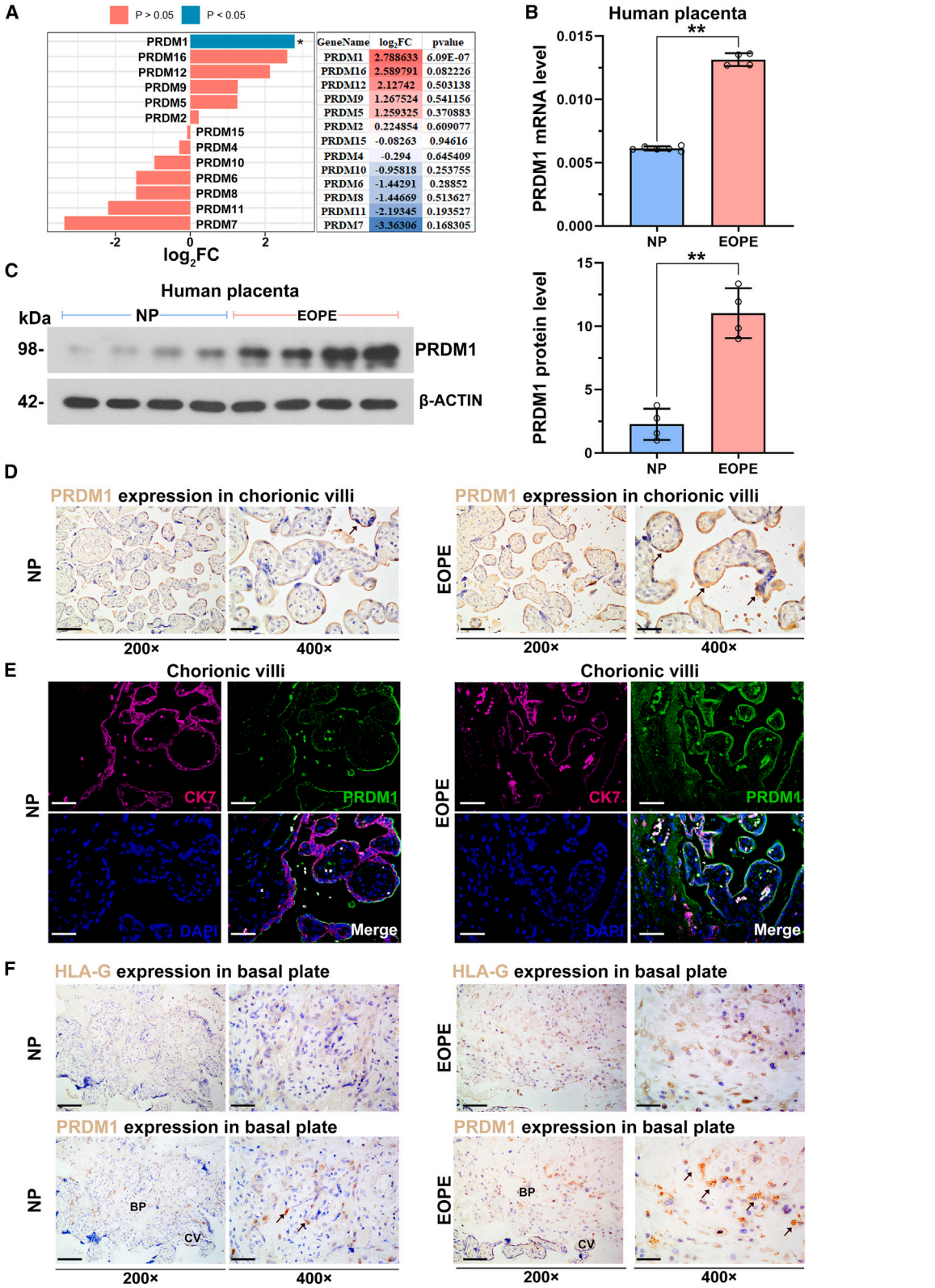

(legend on next page)

was predominately expressed by differentiated trophoblasts (syncytial trophoblasts and invasive trophoblasts). These data indicate that increased PRDM1 may be associated with PE pathogenesis.

The establishment of L-NAME-induced PE-like symptoms

L-NAME-induced PE-like model in rats was established, and two clinical conditions were detected. Compared to pregnant rats treated with saline, rats administrated with L-NAME showed increased urine protein (Figure 3B). Animals treated with L-NAME showed sustained elevated BP values from day 14 to day 20, which was significantly higher than the control group. The observed change indicated that the PE-like model showed similar clinical findings in PE. In order to delve deeper into the pregnancy outcomes of L-NAME-induced rats, we determined the placental and fetal weight. The fetal and placental weights were decreased in the L-NAME group compared to the N.S. group (Figure 3C). Next, we investigated the effect of L-NAME administration on trophoblast cell apoptosis in the placentas by TUNEL staining assay. L-NAME induced a marked increase in TUNEL-positive cells (Figure 3D), indicating that L-NAME resulted in apoptosis in rat placentas. A larger percentage of apoptotic trophoblast cells were observed in the L-NAME group ($p < 0.05$).

PRDM1 expression in placental tissues from Sprague-Dawley rats with L-NAME-induced PE-like symptoms

Given that PRDM1 was highly expressed in the placental tissues of patients with PE, we further evaluated its expression in L-NAME-treated rats. Consistent with expression in human placentas, the mRNA and protein levels of PRDM1 were significantly increased in the placentas of L-NAME-treated rats (Figure 4A). The immunohistochemistry analysis indicated that PRDM1 was highly expressed in placental tissues following L-NAME treatment (Figure 4B). To confirm the PRDM1 expression in the placenta, we performed colocalization of PRDM1 and CK7 or HLA-G in placental tissues with the immunofluorescence assay (Figure 4C). The results confirmed that PRDM1 was expressed in the CK7-labeled trophoblast, and HLA-G-labeled EVTs suggested that PRDM1 might be involved in the regulation of trophoblast function.

Effect of PRDM1 on the proliferation and apoptosis ability of trophoblast cells

Given the elevated PRDM1 expression in STBs and EVTs in EOPE tissues, we investigated its impact on trophoblast cell behavior using the human primary trophoblast and the first-trimester human EVT-derived cell line HTR-8/SVneo. PRDM1 expression was detected by real-time PCR and western blot analyses in trophoblast cells. The exposure to H/R led to an increase in PRDM1 levels, compared to cells exposed to normoxia in both protein and mRNA levels (Figures 5A and S2A). To further determine the effect of PRDM1 on trophoblast *in vitro*, adenoviruses containing PRDM1 encoding fragment or shRNA were constructed to overexpress and silence PRDM1 expression in human primary trophoblastic cells and HTR-8/SVneo cells (Figures S5B–S5D).

Normal proliferation and invasion of trophoblasts are considered necessary in pregnancy, and the dysregulation of placental trophoblasts occurs during PE.[30] The effect of PRDM1 on the growth and invasion was detected in isolated primary trophoblast cells. The exposure to H/R led to a significant inhibition in cell viability and promoted apoptosis of primary trophoblast cells. These changes were attenuated by PRDM1 knockdown (Figures 5B and 5C). In human primary trophoblast cells, the invasiveness and migration abilities were decreased under the H/R conditions, and H/R-inhibited invasiveness was reversed by the inhibition of PRDM1 (Figure 5D).

HTR-8/SVneo cells were used for further verification of the effect of PRDM1 on trophoblast function. It has been indicated that HTR-8/SVneo cells were exposed to low O_2, in which they migrate and proliferate.[31] Consistently, the exposure to H/R of HTR-8/SVneo cells exhibited decreased cell proliferation and migration. Inhibition of PRDM1 promoted proliferation and inhibited apoptosis of trophoblast cells (Figures S2B–S2D). Moreover, PRDM1 overexpression impaired HTR-8/SVneo cell growth and invasion under normoxia (Figures S2E–S2G).

Increased expression of CREBBP in placental tissues of patients with PE and Sprague-Dawley rats treated with L-NAME

To explore whether the CREB-related genes participated in the pathophysiology of PE, we analyzed the expression levels of CREBBP and EP300. Interestingly, in clinical PE placentas, CREBBP expression was upregulated ($\log_2FC = 1.364$; $p = 0.0005$), while EP300 expression was not changed (Figure S3A). Real-time PCR and western blot results verified results from RNA-seq (Figures S3B and S3C). Consistently, CREBBP expression in the placentas of L-NAME-treated rats was increased as well (Figures S3D and S3E). These findings indicate an abnormal upregulation of CREBBP, but not its important ortholog EP300, in both murine and human PE placentas.

Figure 2. PRDM1 expression in placentas from EOPE and healthy pregnant women

(A) A total of 13 PRDM members were identified via high-throughput transcriptome sequencing. Graph showing gene expression between groups. p value < 0.05 and $|\log_2FC| > 1$ were considered significant.

(B) The mRNA expression of PRDM1 in placentas was detected by real-time PCR (EOPE; $n = 4$; NP; $n = 6$).

(C) Representative western blots of PRDM1 from four patients with EOPE and the healthy controls in placentas (left); the quantified relative gene expression levels of PRDM1 (right) ($n = 4$).

(D) The localization and expression of PRDM1 in villous were analyzed by immunohistology. Photographs were obtained at 200× and 400× magnification. Scale bar: 100 and 50 μm.

(E) Double immunofluorescence staining of term human placenta tissue indicated nuclear expression and colocalization of PRDM1 to the CK7, marker for trophoblast cells. Nuclei were counterstained with DAPI. Scale bar: 50 μm.

(F) The localization and expression of HLA-G (marker for EVTs) and PRDM1 basal plate were analyzed by immunohistology. Photographs were obtained at 200× and 400× magnification. Scale bar: 100 and 50 μm. Data are presented as mean ± SD. **, $p < 0.01$, EOPE vs. NP. CV, chorionic villi; BP, basal plate.

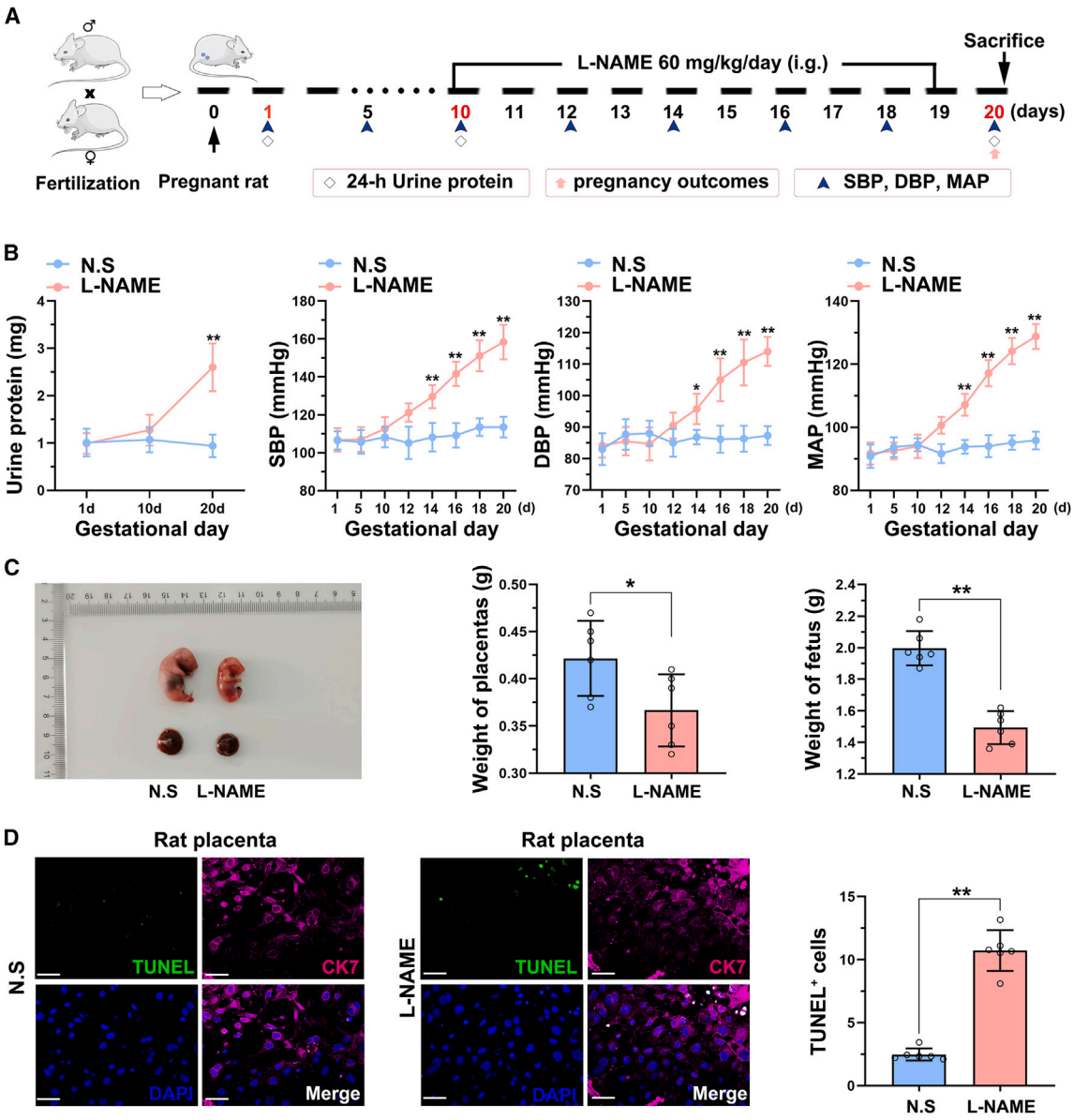

Figure 3. Pregnancy outcomes in pregnant rats exposed to L-NAME

(A) Experimental design of protocol. Schematic chart of the procedures, treatments, and study groups over time.

(B) Comparison of urine protein concentration, systolic blood pressure (SBP), diastolic blood pressure (DBP), and mean arterial pressure (MAP) values between rats treated with L-NAME and vehicle (N.S.). Urine protein concentration was measured on days 1, 10, and 20 post gestation; Blood pressure measurements were evaluated on days 1, 5, 10, 12, 14, 16, 18, and 20 of gestation (n = 6).

(C) Representative images of fetuses and placenta from different treated groups. Fetal and placental weights from different treated groups at 20 days of gestation (n = 6).

(D) Representative images of TUNEL staining in placenta from different groups and quantification for TUNEL+/CK7+ double-stained cells (n = 6). Scale bar: 50 μm. Data are presented as mean ± SD. **p < 0.01, L-NAME vs. N.S.

Effect of CREBBP on the growth and invasion of trophoblast cells exposed to H/R

The results demonstrated that CREBBP expression was remarkably elevated in H/R-cultured trophoblast cells (Figure S4A). To further verify the role of CREBBP, we knocked CREBBP down in trophoblast cells (Figure S5E). Correspondingly, H/R-treated cells displayed reduced viability, increased apoptosis, and decreased invasion and migration, as indicated by CCK-8 (Figure S4B), flow cytometry assay (Figure S4C), and Transwell assay (Figure S4D). SGC-CBP30 is a potent inhibitor of CREBBP[32] and was used to deactivate CREBBP. Consistent with the genetic knockdown of CREBBP, inhibition of CREBBP by SGC-CBP30 treatment markedly increased cell growth and migration. We then focused on matrix metalloproteinase (MMP)

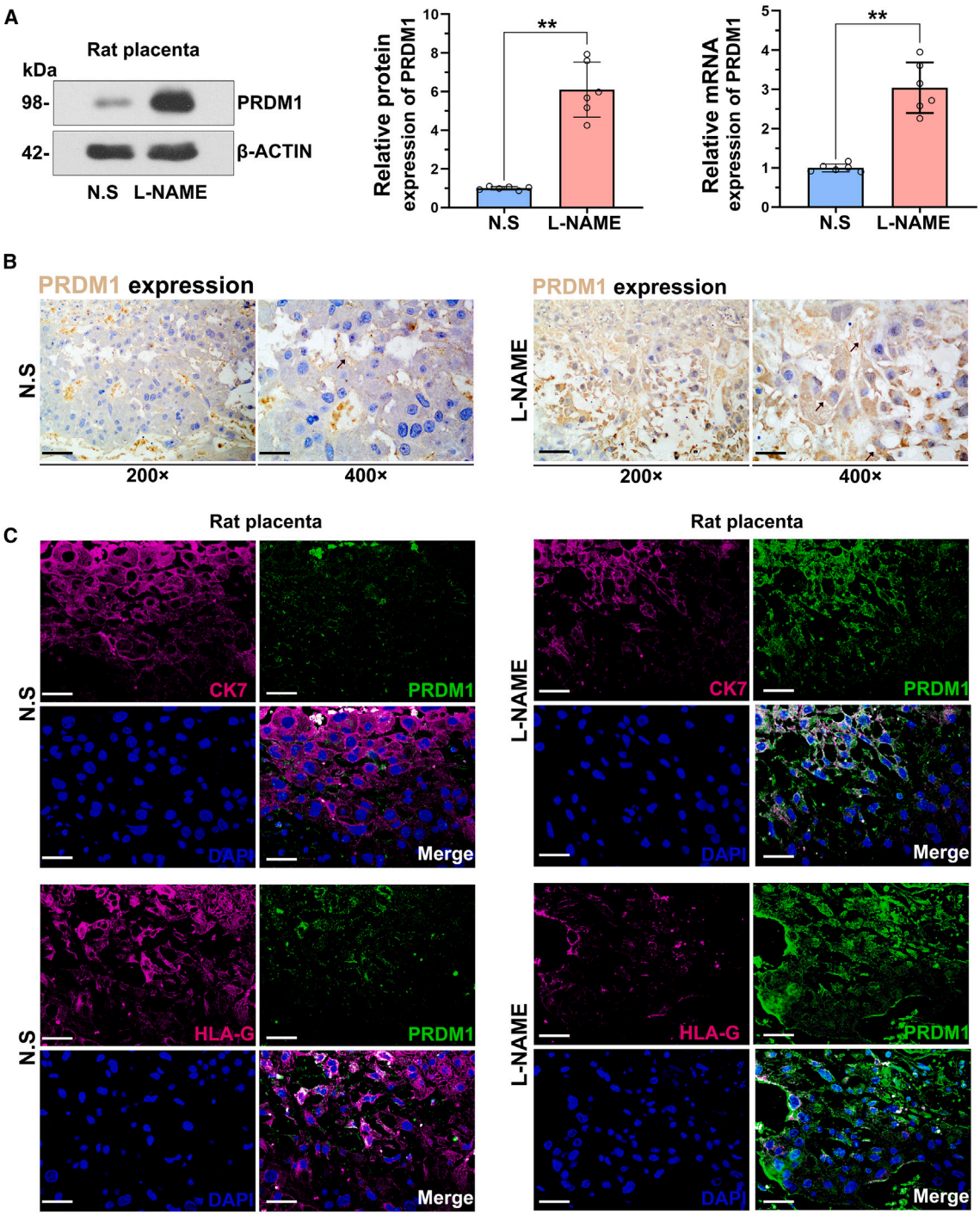

Figure 4. Upregulation of PRDM1 in the placentas of L-NAME-treated Sprague-Dawley rats

(A) Relative protein and mRNA expression of PRDM1 in placentas were detected by western blot analysis and real-time PCR ($n = 6$).

(B) Representative images of immunohistochemical staining for PRDM1 in placenta tissues. Photographs were obtained at 200× and 400× magnification. Scale bar: 100 and 50 μm.

(C) Double immunofluorescence staining of rat placental tissue indicated nuclear expression and colocalization of PRDM1 to the CK7 and HLA-G. Nuclei were counterstained with DAPI. Scale bar: 50 μm. Data are presented as mean ± SD. $^{**}p < 0.01$, L-NAME vs. N.S.

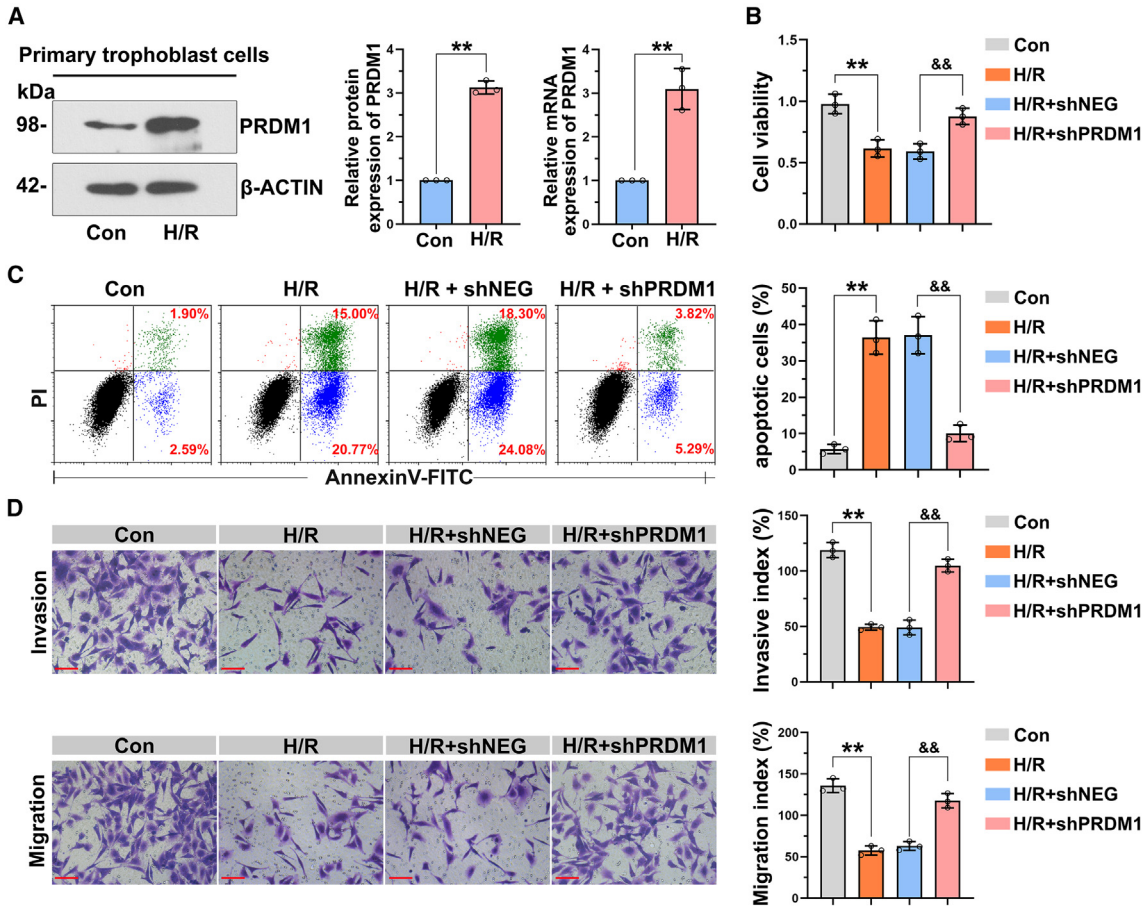

Figure 5. Effect of PRDM1 silencing on growth and invasion of isolated primary trophoblasts

(A) Relative protein and mRNA expression of PRDM1 in isolated primary trophoblasts (n = 3).

(B) CCK-8 assay was implemented to detect cell viability (n = 3).

(C) Cell apoptosis was measured using Annexin V-FITC assays and flow cytometry (n = 3).

(D) Transwell detection revealed the invasion and migration capability of isolated primary trophoblasts (n = 3). Scale bar: 100 μm. Data are presented as mean ± SD. $^{**}p < 0.01$, H/R vs. Con; $^{\&\&}p < 0.01$, H/R + shPRDM1 vs. H/R + shNEG.

2 and MMP9 to analyze migration and invasion abilities (Figure S4E). Importantly, the protein levels of MMP2 and MMP9 were upregulated in response to the inhibition of CREBBP. These findings suggest that CREBBP deficiency promotes the migration and invasion of trophoblast cells after H/R exposure.

PRDM1 regulates cell growth and invasion by regulating CREBBP

Pearson correlation indicated that PRDM1's expression was positively associated with CREBBP's expression (r^2 = 0.729, p = 0.002; Figure 6A). Dual-luciferase results indicated that the activity of CREBBP promoter was significantly increased following the overexpression of PRDM1 (Figure 6B). Next, the conserved binding site of PRDM1 on CREBBP promoter predicted via JASPAR database and three putative binding sites were found (termed site 1, site 2, and site 3). Chromatin immunoprecipitation (ChIP)-PCR was carried out using three sets of CREBBP primers. As indicated in Figure 6C, H/R treatment increased the binding of PRDM1 to CREBBP promoter at sites 1 and 3, but not site 2. Oligonucleotide pull-down assay further verified that the binding of PRDM1 to sites 1 and 3 of CREBBP promoter was increased after H/R treatment (Figure 6D). Furthermore, we found that downregulation of PRDM1 markedly decreased the expression of CREBBP in trophoblast cells (Figure 6E). These results indicate CREBBP as a direct target of PRDM1 in trophoblast cells under H/R condition.

To explore whether PRDM1 exerted its function through the regulation of CREBBP, we silenced CREBBP expression in PRDM1-overexpressed trophoblast cells. We found that knockdown of CREBBP significantly abrogated the PRDM1 overexpression-induced alterations (Figure 7). Taken together, these results suggested that PRDM1 negatively regulated trophoblast cell proliferation and invasion through CREBBP.

DISCUSSION

During normal pregnancy, interstitial trophoblasts migrate toward the uterine spiral arteries and luminal structure in the

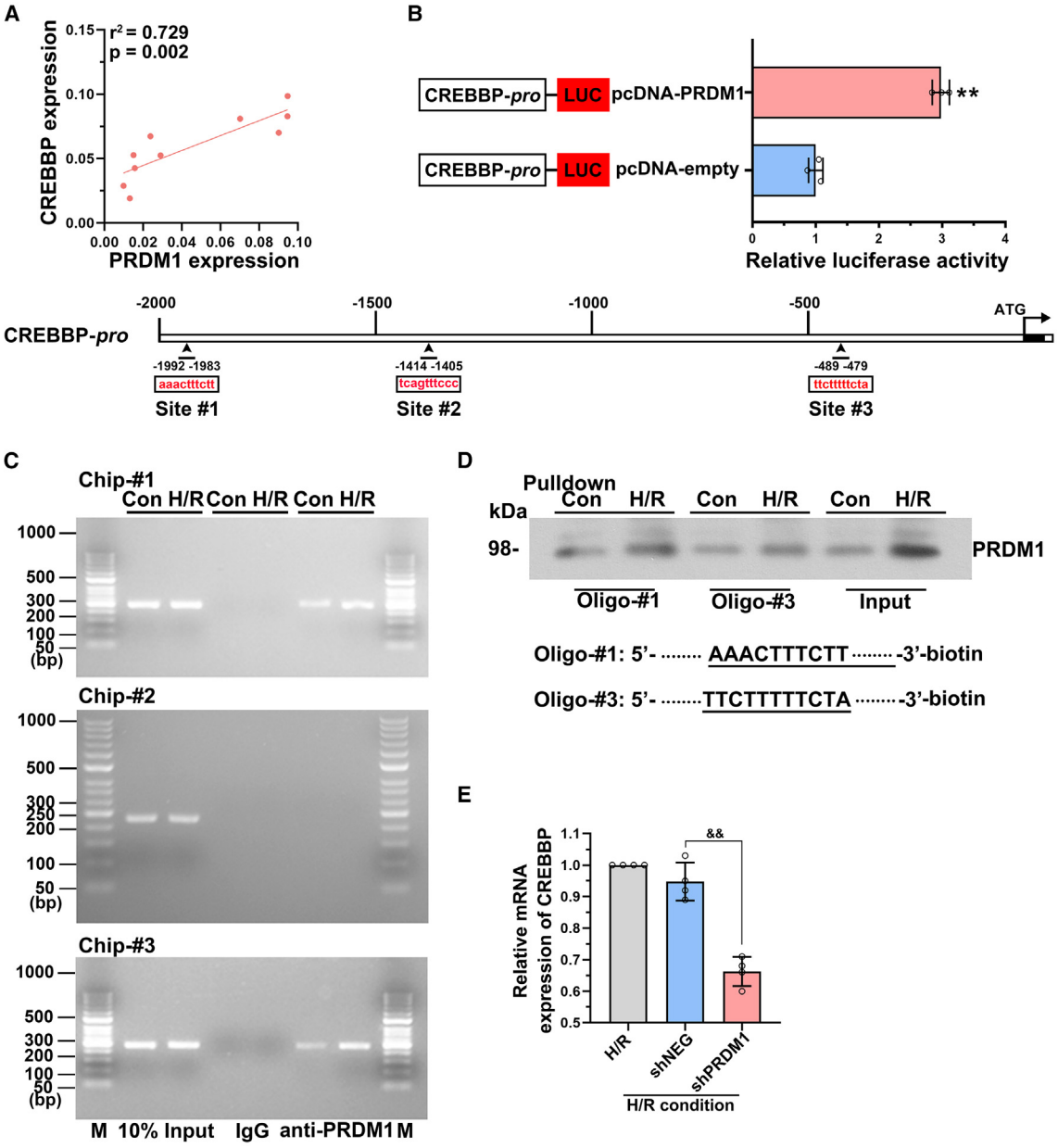

Figure 6. H/R promotes the binding of PRDM1 to CREBBP's promoter

(A) The correlation between PRDM1 and CREBBP expression was detected by Pearson's correlation.

(B) HEK293 cells were co-transfected with indicated plasmids. Luciferase activity was determined.

(C) ChIP assays were carried out, and the CREBBP promoter regions containing PRDM1-binding sites 1, 2, and 3 were amplified by PCR.

(D) Oligonucleotide pull-down assay was performed by using biotinylated double-stranded oligonucleotide probes. DNA proteins were analyzed by western blot with an anti-PRDM1 antibody.

(E) The mRNA expression of CREBBP in trophoblast cells was detected by real-time PCR ($n = 3$). Data are presented as mean ± SD. $^{**}p < 0.01$, pcDNA-empty vs. pcDNA-PRDM1; $^{\&\&}p < 0.01$, H/R + shPRDM1 vs. H/R + shNEG.

placental bed.[33,34] Successful remodeling of the maternal spiral arteries requires sufficient invasion of trophoblast.[35] Identification of potential candidates responsible for impaired trophoblast invasion will shed light on PE treatment. Results from RNA-seq analysis showed potential candidates related to EOPE development, including the previously unrecognized family members. Among detectable PRDMs in placentas, only PRDM1 showed a significant upregulation in preeclamptic placentas, drawing our attention. The upregulated PRDM1 expression in placental samples demonstrated its predictive value for diagnosing PE in early pregnancy. To confirm whether PRDM1 level was elevated in PE cases, we analyzed PRDM1 expression using large-scale

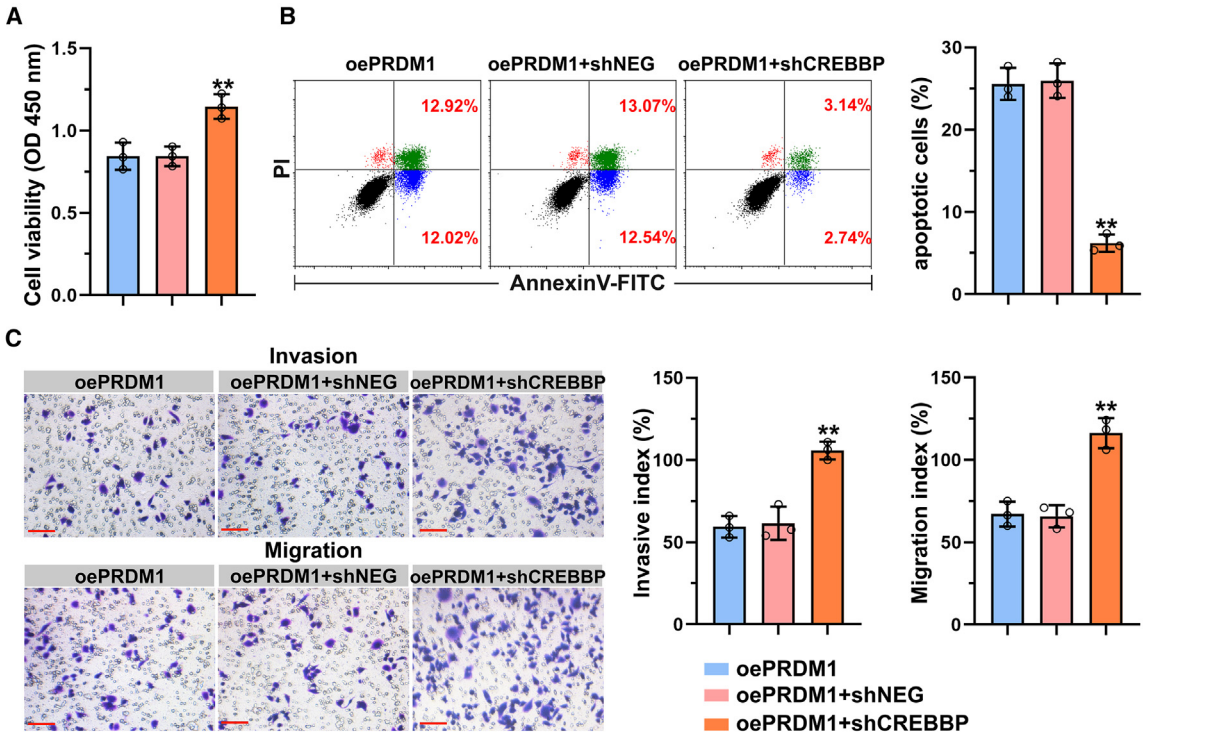

Figure 7. Knockdown of CREBBP abrogated PRDM1 overexpression-mediated alterations of trophoblasts

We silenced CREBBP expressing in PRDM1-overexpressed trophoblast cells.

(A–C) CCK-8 assay ($n = 3$), Annexin V-FITC assays ($n = 3$), and Transwell detection in HTR-8/SVneo cells ($n = 3$). Scale bar: 100 μm. Data are presented as mean ± SD. $^{**}p < 0.01$, oePRDM1 + shCREBBP vs. oePRDM1 + shNEG.

cohorts from other research teams. Consistently, the expression of PRDM1 was also upregulated in placental tissues of patients with EOPE compared to normotensive controls from datasets GSE149812 and GSE177049. These data together strengthen the notion that PRDM1 is one of the potential targets of PE.

There are several animal models that can be used to replicate clinical PE. L-NAME is an inhibitor of nitric oxide synthase, and the administration of L-NAME can induce increased blood pressure, proteinuria, and impairment of placental morphology in the pregnant murine.[36] Moreover, L-NAME increases the apoptosis in the placental bed of pregnant rats.[37] Gravid and non-pregnant rats demonstrated a similar response to L-NAME infusion.[38] Although both groups demonstrate a PE-like phenotype, the presence of hypertension, proteinuria, and apoptosis in virgins contradicts the main assumption of the diagnosis of PE, as it is reserved for the gestational period.[39] Our results showed that, in addition to inducing PE-like phenotype in Sprague-Dawley rats, L-NAME increased placental PRDM1 expression at both transcriptional and translational levels. Such results together with the data derived from clinical samples suggest a link between high PRDM1 expression and PE development. A previous study found that PRDM1 was expressed in proliferative trophoblasts, fetal endothelial cells of the labyrinth, as well as undefined cell types of maternal origin within the decidua.[21] In PE, several cell types such as EVTs and vascular endothelial cells are supposed to be involved in the pathogenic processes.[40] In the current study, we demonstrated that PRDM1 was mainly expressed in the STBs and EVTs in the placenta of patients with PE and L-NAME-treated rats. Based on this, our subsequent experiments focus on functional roles, including the invasion and migration capacities of trophoblast cells, irrespective of the villous or extravillous.

The relationship between abnormal placental development and PE is complex. Trophoblasts, important functional cells in the placenta, play important roles in maintaining placental function.[41] Regulation of the key events of trophoblasts, including proliferation, invasion, and apoptosis, is essential for successful placentation and pregnancy outcome.[42] Oncological studies demonstrated that PRDM1 expression is associated with cancer cell growth and invasion, suggesting that PRDM1 may play a unique role in promoting cell viability and migration.[19,43] These findings are consistent with our observations, suggesting that PRDM1 enhances trophoblast cell's ability to proliferate and migrate. The level of placental oxygen varies with gestation.[44] It has been demonstrated that trophoblasts submitted to low/high O_2 changes, exhibited oxidative stress, and associated with reduced migration.[31] H/R model *in vitro* was performed to mimic the molecular modifications observed in placentas from pathological pregnancy.[45] *In vitro*, the downregulation of PRDM1 in trophoblast cells perturbed the proliferative, migratory, and invasive ability, suggesting that PRDM1 might be necessary for the regulation of basic cellular functions likely early in gestation.

Exploring trophoblast invasion relies on a suitable trophoblast line because obtaining pure, primary, first-trimester human trophoblast remains a challenge. Several trophoblast cell lines have been developed to study trophoblast function *in vitro*. Neither of the available trophoblast cell lines[46] represent the physiological conditions since these are either choriocarcinoma-derived or immortalized by transformation of human EVT cells. In the current study, we proposed a cell model for PE using isolated primary trophoblast cells from healthy pregnancies and the EVT-derived cell line HTR-8/SVneo. The HTR-8/SVneo cell line was established by infecting human first-trimester EVTs with SV40 large T antigen and is a common cell model for studying the biology of EVTs.[47] It has been indicated that the HTR-8/SVneo cell line has a first-trimester origin with invasive EVT phenotype.[48] In addition, the HTR8/SVneo cell line is commonly used as a model for migration/invasion studies for invasive EVT characteristics.[49–52] Although the HTR-8/SVneo cell line is not a valid model system for human trophoblast, these cells exhibit a high proliferation index and share numerous phenotypic similarities with the parental trophoblast cells.[53,54] The present study mainly explored the functional effects of PRDM1 on trophoblast cell invasion and migration. Interestingly, PRDM1 expression was upregulated in trophoblast cells post H/R, and its knockdown prevented H/R-induced cellular damage. These findings confirmed an association of elevated PRDM1 with poor trophoblast function. Our study depicting the potential role of PRDM1 adds information in this area.

CREBBP is a ubiquitously expressed transcriptional coactivator and a lysine acetyltransferase.[22] Unlike EP300, the expression of CREBBP was upregulated in placental tissues from patients with PE. Pharmacological inhibition of CREBBP increased MMP9 and MMP2 expression in mice liver.[55] We further demonstrated the inhibitory role of CREBBP in trophoblast cell invasion by treating with its antagonist SGC-CBP30 or directly knocking CREBBP down with shRNA. A positive correlation of CREBBP and PRDM1 was found in the analyzed placentas. PRDM1 is a transcriptional regulator, and there are three potential regions on CREBBP predicated to contain PRDM1-binding sites. The interesting results revealing a positive correlation between PRDM1 and CREBBP inspired us to dig more into the underlying mechanisms. H/R treatment not only increased the expression levels of PRDM1 and CREBBP but also augmented their interaction. PRDM1 affected trophoblast cell survival and invasion in a CREBBP-dependent manner.

In sum, our work reveals that the activated PRDM1-CREBBP axis may contribute to trophoblast dysfunction and subsequent abnormal placenta development associated with PE pregnancies. Overall, our study reports that altered placental PRDM1 is one of the results of the underlying cause of poor placentation.

Limitations of the study

In the present study, we identified the transcriptome alterations in four placental tissues from patients with EOPE. Although the results revealed the dysregulation of PRDM1 in PE, it was limited by the small number of samples and the major differences in gestational age and fetal growth trajectories of samples. In addition, whether elevated PRDM1 independently induced PE-like features has not been investigated in the current study. We will continue collecting more suitable clinical samples, conducting a follow-up study of these patients with PE, and sharing the obtained data in the future. In addition, in our design, we focused on EOPE with FGR using selected specimens that we believed would represent cases with the greatest potential to benefit from further targeted research; however, this restriction did not allow us to explore other clinical manifestations of these conditions. A subset of patients develop EOPE together with FGR, suggesting an overlap in the etiology underlying these complications.[56] The placenta is a heterogeneous and complex organ. There are many factors surrounding sample collection that can influence subsequent analyses obtained from the human placenta. In the present study, full-term uncomplicated placentas were defined as controls, which is the expected biologically normal event. However, it is beneficial to compare placental samples of similar gestational age because of the prime consideration of comparing placental tissues that are of similar developmental stages. The inclusion of both preterm and term controls may be beneficial for understanding how selection of the control samples impacts results.

RESOURCE AVAILABILITY

Lead contact

Further information and requests for resources and reagents should be directed to and will be fulfilled by the lead contact, Dr. Lei Sun (SJFCK189@163.com).

Materials availability

This study did not generate new unique reagents.

Data and code availability

- The raw data derived from RNA-seq analysis have been deposited in the NCBI Gene Expression Omnibus repository and are publicly available as of the date of publication. Accession numbers are listed in the key resources table.
- This study does not report original code.
- Any additional information required to reanalyze the data reported in this paper is available from the lead contact upon request.

ACKNOWLEDGMENTS

This study was supported by the Science and Technology Plan Project of Liaoning Province (2023-MS-171).

AUTHOR CONTRIBUTIONS

Conceptualization, X.Z. and L.S.; methodology, formal analysis, investigation, writing – original draft, and writing – review and editing, X.Z. and L.S.; funding acquisition, X.Z. All authors read, corrected, and approved the final manuscript.

DECLARATION OF INTERESTS

The authors declare no competing interests.

STAR★METHODS

Detailed methods are provided in the online version of this paper and include the following:

- KEY RESOURCES TABLE
- EXPERIMENTAL MODEL AND STUDY PARTICIPANT DETAILS
  - Animal

SUPPLEMENTAL INFORMATION

Supplemental information can be found online at https://doi.org/10.1016/j.isci.2024.111484.

Received: January 18, 2024
Revised: August 15, 2024
Accepted: November 25, 2024
Published: December 3, 2024

REFERENCES

1. Ives, C.W., Sinkey, R., Rajapreyar, I., Tita, A.T.N., and Oparil, S. (2020). Preeclampsia-Pathophysiology and Clinical Presentations: JACC State-of-the-Art Review. J. Am. Coll. Cardiol. *76*, 1690–1702. https://doi.org/10.1016/j.jacc.2020.08.014.
2. Rana, S., Lemoine, E., Granger, J.P., and Karumanchi, S.A. (2019). Preeclampsia: Pathophysiology, Challenges, and Perspectives. Circ. Res. *124*, 1094–1112. https://doi.org/10.1161/circresaha.118.313276.
3. Staff, A.C., Fjeldstad, H.E., Fosheim, I.K., Moe, K., Turowski, G., Johnsen, G.M., Alnaes-Katjavivi, P., and Sugulle, M. (2022). Failure of physiological transformation and spiral artery atherosis: their roles in preeclampsia. Am. J. Obstet. Gynecol. *226*, S895–s906. https://doi.org/10.1016/j.ajog.2020.09.026.
4. Zadora, J., Singh, M., Herse, F., Przybyl, L., Haase, N., Golic, M., Yung, H.W., Huppertz, B., Cartwright, J.E., Whitley, G., et al. (2017). Disturbed Placental Imprinting in Preeclampsia Leads to Altered Expression of DLX5, a Human-Specific Early Trophoblast Marker. Circulation *136*, 1824–1839. https://doi.org/10.1161/circulationaha.117.028110.
5. Herzog, E.M., Eggink, A.J., Willemsen, S.P., Slieker, R.C., Wijnands, K.P.J., Felix, J.F., Chen, J., Stubbs, A., van der Spek, P.J., van Meurs, J.B., and Steegers-Theunissen, R.P.M. (2017). Early- and late-onset preeclampsia and the tissue-specific epigenome of the placenta and newborn. Placenta *58*, 122–132. https://doi.org/10.1016/j.placenta.2017.08.070.
6. Boss, A.L., Chamley, L.W., and James, J.L. (2018). Placental formation in early pregnancy: how is the centre of the placenta made? Hum. Reprod. Update *24*, 750–760. https://doi.org/10.1093/humupd/dmy030.
7. Abbas, Y., Turco, M.Y., Burton, G.J., and Moffett, A. (2020). Investigation of human trophoblast invasion in vitro. Hum. Reprod. Update *26*, 501–513. https://doi.org/10.1093/humupd/dmaa017.
8. Burton, G.J., Woods, A.W., Jauniaux, E., and Kingdom, J.C.P. (2009). Rheological and physiological consequences of conversion of the maternal spiral arteries for uteroplacental blood flow during human pregnancy. Placenta *30*, 473–482. https://doi.org/10.1016/j.placenta.2009.02.009.
9. Turco, M.Y., and Moffett, A. (2019). Development of the human placenta. Development *146*, dev163428. https://doi.org/10.1242/dev.163428.
10. Huppertz, B. (2018). The Critical Role of Abnormal Trophoblast Development in the Etiology of Preeclampsia. Curr. Pharmaceut. Biotechnol. *19*, 771–780. https://doi.org/10.2174/1389201019666180427110547.
11. Staun-Ram, E., and Shalev, E. (2005). Human trophoblast function during the implantation process. Reprod. Biol. Endocrinol. *3*, 56. https://doi.org/10.1186/1477-7827-3-56.
12. Farah, O., Nguyen, C., Tekkatte, C., and Parast, M.M. (2020). Trophoblast lineage-specific differentiation and associated alterations in preeclampsia and fetal growth restriction. Placenta *102*, 4–9. https://doi.org/10.1016/j.placenta.2020.02.007.
13. Yong, H.E.J., and Chan, S.-Y. (2020). Current approaches and developments in transcript profiling of the human placenta. Hum. Reprod. Update *26*, 799–840. https://doi.org/10.1093/humupd/dmaa028.
14. Cox, B., Leavey, K., Nosi, U., Wong, F., and Kingdom, J. (2015). Placental transcriptome in development and pathology: expression, function, and methods of analysis. Am. J. Obstet. Gynecol. *213*, S138–S151. https://doi.org/10.1016/j.ajog.2015.07.046.
15. Li, Q., Zhang, L., You, W., Xu, J., Dai, J., Hua, D., Zhang, R., Yao, F., Zhou, S., Huang, W., et al. (2022). PRDM1/BLIMP1 induces cancer immune evasion by modulating the USP22-SPI1-PD-L1 axis in hepatocellular carcinoma cells. Nat. Commun. *13*, 7677. https://doi.org/10.1038/s41467-022-35469-x.
16. Yoshikawa, T., Wu, Z., Inoue, S., Kasuya, H., Matsushita, H., Takahashi, Y., Kuroda, H., Hosoda, W., Suzuki, S., and Kagoya, Y. (2022). Genetic ablation of PRDM1 in antitumor T cells enhances therapeutic efficacy of adoptive immunotherapy. Blood *139*, 2156–2172. https://doi.org/10.1182/blood.2021012714.
17. Di Tullio, F., Schwarz, M., Zorgati, H., Mzoughi, S., and Guccione, E. (2022). The duality of PRDM proteins: epigenetic and structural perspectives. FEBS J. *289*, 1256–1275. https://doi.org/10.1111/febs.15844.
18. Guo, H., Wang, M., Wang, B., Guo, L., Cheng, Y., Wang, Z., Sun, Y.Q., Wang, Y., Chang, Y.J., and Huang, X.J. (2022). PRDM1 Drives Human Primary T Cell Hyporesponsiveness by Altering the T Cell Transcriptome and Epigenome. Front. Immunol. *13*, 879501. https://doi.org/10.3389/fimmu.2022.879501.
19. Zeng, F., Luo, L., Li, D., Guo, J., and Guo, M. (2021). KPNA2 interaction with CBX8 contributes to the development and progression of bladder cancer by mediating the PRDM1/c-FOS pathway. J. Transl. Med. *19*, 112. https://doi.org/10.1186/s12967-021-02709-5.
20. Mould, A., Morgan, M.A.J., Li, L., Bikoff, E.K., and Robertson, E.J. (2012). Blimp1/Prdm1 governs terminal differentiation of endovascular trophoblast giant cells and defines multipotent progenitors in the developing placenta. Genes Dev. *26*, 2063–2074. https://doi.org/10.1101/gad.199828.112.
21. Nelson, A.C., Mould, A.W., Bikoff, E.K., and Robertson, E.J. (2016). Single-cell RNA-seq reveals cell type-specific transcriptional signatures at the maternal-foetal interface during pregnancy. Nat. Commun. *7*, 11414. https://doi.org/10.1038/ncomms11414.
22. Dancy, B.M., and Cole, P.A. (2015). Protein lysine acetylation by p300/CBP. Chem. Rev. *115*, 2419–2452. https://doi.org/10.1021/cr500452k.
23. Ali, I., Conrad, R.J., Verdin, E., and Ott, M. (2018). Lysine Acetylation Goes Global: From Epigenetics to Metabolism and Therapeutics. Chem. Rev. *118*, 1216–1252. https://doi.org/10.1021/acs.chemrev.7b00181.
24. Conery, A.R., Centore, R.C., Neiss, A., Keller, P.J., Joshi, S., Spillane, K.L., Sandy, P., Hatton, C., Pardo, E., Zawadzke, L., et al. (2016). Bromodomain inhibition of the transcriptional coactivators CBP/EP300 as a therapeutic strategy to target the IRF4 network in multiple myeloma. Elife *5*, e10483. https://doi.org/10.7554/eLife.10483.
25. Jiang, Y., Ortega-Molina, A., Geng, H., Ying, H.-Y., Hatzi, K., Parsa, S., McNally, D., Wang, L., Doane, A.S., Agirre, X., et al. (2017). CREBBP Inactivation Promotes the Development of HDAC3-Dependent Lymphomas.

Cancer Discov. *7*, 38–53. https://doi.org/10.1158/2159-8290.CD-16-0975.

26. Sadeghi, H., Esmkhani, S., Pirjani, R., Amin-Beidokhti, M., Gholami, M., Azizi Tabesh, G., Ghasemi, M.R., Gachkar, L., and Mirfakhraie, R. (2021). CREB-binding protein (CREBBP) and preeclampsia: a new promising target gene. Mol. Biol. Rep. *48*, 2117–2122. https://doi.org/10.1007/s11033-021-06215-1.

27. van Uitert, M., Moerland, P.D., Enquobahrie, D.A., Laivuori, H., van der Post, J.A.M., Ris-Stalpers, C., and Afink, G.B. (2015). Meta-Analysis of Placental Transcriptome Data Identifies a Novel Molecular Pathway Related to Preeclampsia. PLoS One *10*, e0132468. https://doi.org/10.1371/journal.pone.0132468.

28. Moser, G., Orendi, K., Gauster, M., Siwetz, M., Helige, C., and Huppertz, B. (2011). The art of identification of extravillous trophoblast. Placenta *32*, 197–199. https://doi.org/10.1016/j.placenta.2010.11.008.

29. Dunk, C.E., Bucher, M., Zhang, J., Hayder, H., Geraghty, D.E., Lye, S.J., Myatt, L., and Hackmon, R. (2022). Human leukocyte antigen HLA-C, HLA-G, HLA-F, and HLA-E placental profiles are altered in early severe preeclampsia and preterm birth with chorioamnionitis. Am. J. Obstet. Gynecol. *227*, 641.e1–641.e13. https://doi.org/10.1016/j.ajog.2022.07.021.

30. Harati-Sadegh, M., Kohan, L., Teimoori, B., Mehrabani, M., and Salimi, S. (2019). Analysis of polymorphisms, promoter methylation, and mRNA expression profile of maternal and placental P53 and P21 genes in preeclamptic and normotensive pregnant women. J. Biomed. Sci. *26*, 92. https://doi.org/10.1186/s12929-019-0586-x.

31. Guerby, P., Swiader, A., Augé, N., Parant, O., Vayssière, C., Uchida, K., Salvayre, R., and Negre-Salvayre, A. (2019). High glutathionylation of placental endothelial nitric oxide synthase in preeclampsia. Redox Biol. *22*, 101126. https://doi.org/10.1016/j.redox.2019.101126.

32. Zhu, Y.X., Shi, C.-X., Bruins, L.A., Wang, X., Riggs, D.L., Porter, B., Ahmann, J.M., de Campos, C.B., Braggio, E., Bergsagel, P.L., and Stewart, A.K. (2019). Identification of lenalidomide resistance pathways in myeloma and targeted resensitization using cereblon replacement, inhibition of STAT3 or targeting of IRF4. Blood Cancer J. *9*, 19. https://doi.org/10.1038/s41408-019-0173-0.

33. Pijnenborg, R., Vercruysse, L., and Hanssens, M. (2006). The uterine spiral arteries in human pregnancy: facts and controversies. Placenta *27*, 939–958. https://doi.org/10.1016/j.placenta.2005.12.006.

34. Moser, G., Windsperger, K., Pollheimer, J., de Sousa Lopes, S.C., and Huppertz, B. (2018). Human trophoblast invasion: new and unexpected routes and functions. Histochem. Cell Biol. *150*, 361–370. https://doi.org/10.1007/s00418-018-1699-0.

35. Burton, G.J., Redman, C.W., Roberts, J.M., and Moffett, A. (2019). Pre-eclampsia: pathophysiology and clinical implications. Br. Med. J. *366*, l2381. https://doi.org/10.1136/bmj.l2381.

36. de Alwis, N., Binder, N.K., Beard, S., Mangwiro, Y.T., Kadife, E., Cuffe, J.S., Keenan, E., Fato, B.R., Kaitu'u-Lino, T.J., Brownfoot, F.C., et al. (2022). The L-NAME mouse model of preeclampsia and impact to long-term maternal cardiovascular health. Life science alliance *5*, e202201517. https://doi.org/10.26508/lsa.202201517.

37. Suzuki, T., Nagamatsu, C., Kushima, T., Miyakoshi, R., Tanaka, K., Morita, H., Sakaue, M., and Takizawa, T. (2010). Apoptosis caused by an inhibitor of NO production in the decidua of rat from mid-gestation. Exp. Biol. Med. *235*, 455–462. https://doi.org/10.1258/ebm.2009.009285.

38. Danielson, L.A., and Conrad, K.P. (1995). Acute blockade of nitric oxide synthase inhibits renal vasodilation and hyperfiltration during pregnancy in chronically instrumented conscious rats. J. Clin. Invest. *96*, 482–490. https://doi.org/10.1172/jci118059.

39. Sakowicz, A., Bralewska, M., Kamola, P., and Pietrucha, T. (2022). Reliability of Rodent and Rabbit Models in Preeclampsia Research. Int. J. Mol. Sci. *23*, 14344. https://doi.org/10.3390/ijms232214344.

40. Opichka, M.A., Rappelt, M.W., Gutterman, D.D., Grobe, J.L., and McIntosh, J.J. (2021). Vascular Dysfunction in Preeclampsia. Cells *10*, 3055. https://doi.org/10.3390/cells10113055.

41. Aplin, J.D., and Jones, C.J.P. (2021). Cell dynamics in human villous trophoblast. Hum. Reprod. Update *27*, 904–922. https://doi.org/10.1093/humupd/dmab015.

42. Huppertz, B. (2019). Traditional and New Routes of Trophoblast Invasion and Their Implications for Pregnancy Diseases. Int. J. Mol. Sci. *21*, 289. https://doi.org/10.3390/ijms21010289.

43. Sciortino, M., Camacho-Leal, M.D.P., Orso, F., Grassi, E., Costamagna, A., Provero, P., Tam, W., Turco, E., Defilippi, P., Taverna, D., and Cabodi, S. (2017). Dysregulation of Blimp1 transcriptional repressor unleashes p130Cas/ErbB2 breast cancer invasion. Sci. Rep. *7*, 1145. https://doi.org/10.1038/s41598-017-01332-z.

44. Torres-Cuevas, I., Parra-Llorca, A., Sánchez-Illana, A., Nuñez-Ramiro, A., Kuligowski, J., Cháfer-Pericás, C., Cernada, M., Escobar, J., and Vento, M. (2017). Oxygen and oxidative stress in the perinatal period. Redox Biol. *12*, 674–681. https://doi.org/10.1016/j.redox.2017.03.011.

45. Sagrillo-Fagundes, L., Assunção Salustiano, E.M., Ruano, R., Markus, R.P., and Vaillancourt, C. (2018). Melatonin modulates autophagy and inflammation protecting human placental trophoblast from hypoxia/reoxygenation. J. Pineal Res. *65*, e12520. https://doi.org/10.1111/jpi.12520.

46. Hannan, N.J., Paiva, P., Dimitriadis, E., and Salamonsen, L.A. (2010). Models for study of human embryo implantation: choice of cell lines? Biol. Reprod. *82*, 235–245. https://doi.org/10.1095/biolreprod.109.077800.

47. Graham, C.H., Hawley, T.S., Hawley, R.G., MacDougall, J.R., Kerbel, R.S., Khoo, N., and Lala, P.K. (1993). Establishment and characterization of first trimester human trophoblast cells with extended lifespan. Exp. Cell Res. *206*, 204–211. https://doi.org/10.1006/excr.1993.1139.

48. Jeyarajah, M.J., Jaju Bhattad, G., Kops, B.F., and Renaud, S.J. (2019). Syndecan-4 regulates extravillous trophoblast migration by coordinating protein kinase C activation. Sci. Rep. *9*, 10175. https://doi.org/10.1038/s41598-019-46599-6.

49. Canfield, J., Arlier, S., Mong, E.F., Lockhart, J., VanWye, J., Guzeloglu-Kayisli, O., Schatz, F., Magness, R.R., Lockwood, C.J., Tsibris, J.C.M., et al. (2019). Decreased LIN28B in preeclampsia impairs human trophoblast differentiation and migration. Faseb. J. *33*, 2759–2769. https://doi.org/10.1096/fj.201801163R.

50. Walker, O.S., Gurm, H., Sharma, R., Verma, N., May, L.L., and Raha, S. (2021). Delta-9-tetrahydrocannabinol inhibits invasion of HTR8/SVneo human extravillous trophoblast cells and negatively impacts mitochondrial function. Sci. Rep. *11*, 4029. https://doi.org/10.1038/s41598-021-83563-9.

51. Fuenzalida, B., Kallol, S., Zaugg, J., Mueller, M., Mistry, H.D., Gutierrez, J., Leiva, A., and Albrecht, C. (2022). Primary Human Trophoblasts Mimic the Preeclampsia Phenotype after Acute Hypoxia-Reoxygenation Insult. Cells *11*, 1898. https://doi.org/10.3390/cells11121898.

52. Bolnick, A.D., Bolnick, J.M., Kohan-Ghadr, H.R., Kilburn, B.A., Pasalodos, O.J., Singhal, P.K., Dai, J., Diamond, M.P., Armant, D.R., and Drewlo, S. (2017). Enhancement of trophoblast differentiation and survival by low molecular weight heparin requires heparin-binding EGF-like growth factor. Hum. Reprod. *32*, 1218–1229. https://doi.org/10.1093/humrep/dex069.

53. Ulrich, V., Gelber, S.E., Vukelic, M., Sacharidou, A., Herz, J., Urbanus, R.T., de Groot, P.G., Natale, D.R., Harihara, A., Redecha, P., et al. (2016). ApoE Receptor 2 Mediation of Trophoblast Dysfunction and Pregnancy Complications Induced by Antiphospholipid Antibodies in Mice. Arthritis Rheumatol. *68*, 730–739. https://doi.org/10.1002/art.39453.

54. Chen, Z., Geng, Y., Gao, R., Zhong, H., Chen, J., Mu, X., Chen, X., Zhang, Y., Li, F., and He, J. (2022). Maternal exposure to CeO(2)NPs derails placental development through trophoblast dysfunction mediated by excessive autophagy activation. J. Nanobiotechnol. *20*, 131. https://doi.org/10.1186/s12951-022-01334-8.

55. Osawa, Y., Oboki, K., Imamura, J., Kojika, E., Hayashi, Y., Hishima, T., Saibara, T., Shibasaki, F., Kohara, M., and Kimura, K. (2015). Inhibition of Cyclic Adenosine Monophosphate (cAMP)-response Element-binding Protein (CREB)-binding Protein (CBP)/β-Catenin Reduces Liver Fibrosis in Mice. EBioMedicine *2*, 1751–1758. https://doi.org/10.1016/j.ebiom.2015.10.010.

56. Iwahashi, N., Yamamoto, M., Nanjo, S., Toujima, S., Minami, S., and Ino, K. (2017). Downregulation of indoleamine 2, 3-dioxygenase expression in the villous stromal endothelial cells of placentas with preeclampsia. J. Reprod. Immunol. *119*, 54–60. https://doi.org/10.1016/j.jri.2017.01.003.

57. Martinez-Fierro, M.L., Hernadez-Delgadillo, G.P., Flores-Mendoza, J.F., Alvarez-Zuñiga, C.D., Diaz-Lozano, M.L., Delgado-Enciso, I., Romero-Diaz, V.J., Lopez-Saucedo, A., Rodriguez-Sanchez, I.P., Marino-Martinez, I.A., and Garza-Veloz, I. (2021). Fibroblast Growth Factor Type 2 (FGF2) Administration Attenuated the Clinical Manifestations of Preeclampsia in a Murine Model Induced by L-NAME. Front. Pharmacol. *12*, 663044. https://doi.org/10.3389/fphar.2021.663044.

58. Chen, X., Li, P., Liu, M., Zheng, H., He, Y., Chen, M.-X., Tang, W., Yue, X., Huang, Y., Zhuang, L., et al. (2020). Gut dysbiosis induces the development of pre-eclampsia through bacterial translocation. Gut *69*, 513–522. https://doi.org/10.1136/gutjnl-2019-319101.

59. Yang, Z., Bai, B., Luo, X., Xiao, X., Liu, X., Ding, Y., Zhang, H., Gao, L., Li, J., and Qi, H. (2014). Downregulated Krüppel-like factor 8 is involved in decreased trophoblast invasion under hypoxia-reoxygenation conditions. Reprod. Sci. *21*, 72–81. https://doi.org/10.1177/1933719113488448.

60. Ding, H., Dai, Y., Lei, Y., Wang, Z., Liu, D., Li, R., Shen, L., Gu, N., Zheng, M., Zhu, X., et al. (2019). Upregulation of CD81 in trophoblasts induces an imbalance of Treg/Th17 cells by promoting IL-6 expression in preeclampsia. Cell. Mol. Immunol. *16*, 302–312. https://doi.org/10.1038/s41423-018-0186-9.

61. Kolokol'tsova, T.D., Saburina, N.N., Poltavtseva, P.A., and Sukhikh, G.T. (2015). Isolation and culturing of trophoblasts from human terminal placenta. Bull. Exp. Biol. Med. *158*, 532–536. https://doi.org/10.1007/s10517-015-2802-3.

62. Kaidi, A., Qualtrough, D., Williams, A.C., and Paraskeva, C. (2006). Direct transcriptional up-regulation of cyclooxygenase-2 by hypoxia-inducible factor (HIF)-1 promotes colorectal tumor cell survival and enhances HIF-1 transcriptional activity during hypoxia. Cancer Res. *66*, 6683–6691.

STAR★METHODS

KEY RESOURCES TABLE

REAGENT or RESOURCE	SOURCE	IDENTIFIER
Antibodies		
Anti-S100A16 Antibody	Affinity Biosciences	Cat.# DF4353; RRID: AB_10694280
Anti-cleaved caspase-3 Antibody	Affinity Biosciences	Cat.# AF7022; RRID: AB_2835326
Anti-Bcl-2 Antibody	Affinity Biosciences	Cat.# AF6139; RRID: AB_2835021
Anti-Bax Antibody	Affinity Biosciences	Cat.# AF0120; RRID: AB_2833304
Anti-CaM Antibody	Proteintech	Cat.# 10541-1-AP; RRID: AB_2069442
Anti-CAMKK2 Antibody	Proteintech	Cat.# 11549-1-AP; RRID: AB_2259441
Phospho-CAMKK2 Antibody	Affinity Biosciences	Cat.# AF8136; RRID: AB_2801648
Anti-AMPK Antibody	Affinity Biosciences	Cat.# AF6423; RRID: AB_2835253
Phospho-AMPK Antibody	Affinity Biosciences	Cat.# AF3423; RRID: AB_2834865
Anti-VDAC1 Antibody	Affinity Biosciences	Cat.# AF5478; RRID: AB_ 2837960
Biological samples		
Human placental tissues	Shengjing Hospital of China Medical University (No. 2022PS865K)	NA
Chemicals, peptides, and recombinant proteins		
SGC-CBP30	Yuanye Bio-Technology Co., Ltd	Cat# S81370
L-NAME	Yuanye Bio-Technology Co., Ltd	Cat# S20013
Fetal bovine serum	Tianhang Biotechnology Co., Ltd	Cat# 11011-8611
TRIpure solution	BioTeke	Cat# RP1001
Matrigel gel	Corning	Cat# 356234
Critical commercial assays		
Bicinchoninic acid kit	Beyotime	Cat# P0012
CCK-8 kit	KeyGen	Cat# KGA317
In Situ Cell Death Detection Kit	Roche Diagnostics	Cat# 12156792910
Annexin V-FITC Apoptosis Detection Kit	KeyGen	Cat# KGA108
ChIP Assay Kit	Beyotime	Cat# P2078
ATP Assay Kit	Beyotime	Cat# S0026
Luciferase assay kit	KeyGen Biotech	Cat# KGAF040
Deposited data		
RNA-Seq raw data	This paper	GEO database under accession number GSE255126
Experimental models: Cell lines		
HTR-8/SVneo cell line	iCell	Cat# iCell-h390
Primary trophoblasts	Isolated from placentas	NA
Experimental models: Organisms/strains		
Sprague-Dawley rats	Changzhou Cavens Laboratory Animal Co. LTD	NA

(*Continued on next page*)

Continued

REAGENT or RESOURCE	SOURCE	IDENTIFIER
Oligonucleotides		
qPCR primers: homo PRDM1 forward: 5′- GAACGCCAACAGGAAATA-3′ Reverse: 5′-AAAGTCCCGACAATACCAC-3′ Homo CREBBP forward: 5′- GCATTGATAACAGAGTCCCTA-3′ Reverse: 5′- TCTCCGTCTTCATTTCCAG-3′ Homo EP300 forward: 5′- GGCTGTATCAGAGCGTATT-3′ Reverse: 5′- TGCTGTCTCCCTTGGTC-3′ Rat PRDM1 forward: 5′- CGACCTTAGCGACAACG-3′ Reverse: 5′-TGACCTTTACAGGCACCAG-3′ Rat CREBBP forward: 5′- ATCCTATGGACCTTTCTACC-3′ Reverse: 5′- AGCCACGCATTGTTGA-3′ Rat EP300forward: 5′- CATTGTGCGTCTTCTCG-3′ Reverse: 5′- TCTGGTTTACTTGATAGGGT-3′	This paper	NA
Software and algorithms		
Graphpad Prism 8.0	GraphPad Software	https://www.graphpad.com/scientific-software/prism/
Illumina Novaseq™ 6000 software	Bio-Technology	NA
NanoDrop ND-1000 Bioanalyzer	NanoDrop	NA

EXPERIMENTAL MODEL AND STUDY PARTICIPANT DETAILS

Animal

Female Sprague Dawley (SD) rats (250–300 g) were housed under controlled conditions (12 h light/12 h dark cycle at a constant temperature of 25 ± 1°C). Nitro-*l*-arginine methyl ester (L-NAME) (Yuanye Bio-Technology Co., Ltd, cat# S20013, Shanghai, China), an inhibitor of nitric oxide synthetase, was used to establish the PE model in pregnant animals as previously reported.[57] Female rats were housed with male rats at a ratio of 3:1 overnight. Pregnancy in rats was confirmed by the presence of vaginal spermatozoa.[58] On day 10 of pregnancy, rats were randomly divided into the control group (n = 6) and the L-NAME group (n = 6). Pregnant rats in the L-NAME group were administered intragastrically with L-NAME (60 mg/kg/day) from day 10–19. Pregnant rats in the control group received saline solution (0.9% of NaCl) by intragastric route.

Human subjects

All procedures adhered to the Declaration of Helsinki, and ethical approval was obtained from the Institutional Ethics Committee of Ethics Committee of Shengjing Hospital of China Medical University (No. 2022PS865K). Informed consent was obtained from all patients included in the study. Including well-characterized pregnant women with EOPE (n = 4) and healthy normotensive pregnancies (NP; n = 6) were recruited from the Shengjing Hospital of China Medical University. Each enrolled individual has signed the informed consent. Detailed clinical characteristics including general maternal and neonatal variables were obtained from the clinical records and presented in Table S1. The inclusion criteria included: the diagnostic criteria for PE were defined by systolic blood pressure (SBP) $\geq$ 140 mm Hg or diastolic blood pressure (DBP) $\geq$ 90 mm Hg; proteinuria $\geq$0.3 g per 24 h.[30] Exclusion criteria included major fetal chromosomal or congenital abnormalities, autoimmune diseases, chronic hypertension, cardiovascular and metabolic diseases, multiparous pregnancies, stillbirth, and renal diseases. Normal pregnancy was defined as a pregnancy resulting in a healthy newborn delivered at term with normal blood pressure and no complications.

Cell culture

HTR-8/SVneo cell line was employed for the function analysis *in vitro*. HTR-8/SVneo cells were cultured in RPMI-1640 medium (Solarbio, Beijing, China) containing 10% fetal bovine serum (FBS; Tianhang Biotechnology Co., Ltd, cat# 11011-8611, Zhejiang China). HTR8/SVneo cells were exposed to hypoxia (2% O_2) for 8 h and then with 20% O_2 for 16 h for two cycles as previously reported.[59]

METHOD DETAILS

Study subjects

The clinical information of healthy pregnant women and pregnant women with PE in ages (35 ± 3.95 and 34.25 ± 4.27 years; $p > 0.05$), SBP (118.33 ± 6.02 and 180.75 ± 14.22 mm Hg; $p < 0.001$), DBP (77 ± 9.51 and 109.75 ± 6.95 mm Hg; $p < 0.001$), and proteinuria were listed in Table S2. Chorionic villous tissues and the basal plate of placenta from PE and NP were dissected as previously described.[60] After initial washing with ice-cold PBS, the tissue was cut into thin sections (<3mm) and kept on ice to minimize proteolysis. Slices were washed another 8–10 times until nearly all blood was removed. Villous tissues were stored individually in RNAlater, and placed in a refrigerator at 4°C. Following this, samples were frozen and stored at −80°C until analysis. The transcriptome changes during the progression of PE were further determined using the GSE149812 and GSE177049 datasets based on the Gene Expression Omnibus (GEO, https://www.ncbi.nlm.nih.gov/geo/geo2r/) database.

RNA-seq

Total RNAs were isolated from villus tissue samples with Trizol (Invitrogen, California, USA). RNA concentration was detected with NanoDrop ND-1000 Bioanalyzer (NanoDrop, Wilmington, USA). RNA integrity was determined by Bioanalyzer 2100 (Agilent, Santa Clara, USA). Samples (≥ 1 μg) of RNA integrity number (RIN) $\geq$ 7.0 and OD260/280 $\geq$ 1.8 were subjected to RNA-seq. cDNA library was prepared using the Invitrogen SuperScript II Reverse Transcriptase (Invitrogen, California, USA). RNA-seq was performed on the Illumina Novaseq 6000 (LC Bio-Technology, Hangzhou, China). RNA-Seq raw data have been deposited in the NCBI database (https://www.ncbi.nlm.nih.gov/) under accession GSE255126.

Genes with Log_2 (fold-changes) ≥ 1 or ≤ -1, and P-value ≤ 0.05 were selected as differentially expressed genes (DEGs). The principal component analysis (PCA) was performed with default parameters. Gene Ontology (GO) (http://www.geneontology.org/) enrichment analysis of DEGs was implemented by R package. Functional enrichment of DEGs was determined via Gene Ontology (GO), Kyoto Encyclopedia of Genes and Genomes (KEGG) pathway, and Gene Set Enrichment Analysis (GSEA).

Animal experimental protocol

Figure 3A summarizes the experimental design of the protocol. For the assessment of proteinuria, the 24-h urine samples were collected on days 1, 10, and 20 of the experimental protocol and the protein concentration of each urine sample was determined. Blood pressure measurements were performed in a relatively stable environment during the experimental period. Rats in the protocol experienced blood pressure measurements on days on days 1, 5, 10, 12, 14, 16, 18, and 20 according with to manufacturer's recommendations. SBP, DBP, and arterial pressure (MAP) of pregnant rats in each group were monitored using a non-invasive automated sphygmomanometer. On the 20th day of gestation, animals were anesthetized, and fetuses and placentas were collected. The placentas were weighed and used for subsequent experiments, while the fetuses were weighed and imaged. Placentas were collected and fixed with 4% paraformaldehyde for further analysis. All procedures were approved by the Laboratory Animal Welfare and Animal Care and Use Committee of Shengjing Hospital of China Medical University (No. 2022PS814K).

Isolation of trophoblasts and cell culture

Term placentas were obtained immediately from five uncomplicated pregnancies, and detailed clinical characteristics including general maternal and neonatal variables were obtained from the clinical records and presented in Table S3. This study was approved by the ethical committee of Shengjing Hospital of China Medical University. The primary trophoblasts were isolated following a well-established protocol as previously described.[61] In brief, chorionic villous tissues were thoroughly washed with cold PBS and minced into fragments. Tissue fragments were incubated with enzymatic digestion in a Hanks' Balanced Salt Solution (Invitrogen, CA) solution containing 0.25% trypsin and 0.2 mg/mL DNase I. Cell suspension was separated by density gradient centrifugation in a 5–70% discontinuous Percoll gradient. The collected cells (5×10^5/mL) were cultured in IMDM medium containing 10% FBS and 50 μg/mL gentamicin. Isolated primary trophoblasts were evaluated by staining with specific cells marker cytokeratin-7 (CK7) (Figure S5A). The primary trophoblasts were cultured in the incubator of normoxia conditions (8% O_2, 87% N_2, 5% CO_2) to ensure cell adherence. For creating H/R, cells were exposed to hypoxia (0.5% O_2, 94.5% N_2, 5% CO_2) for 4 h. After anoxia, reoxygenation was initiated by incubation in normoxic conditions for 18 h as previously reported.[45] Short hairpin RNA (shRNA) targeting PRDM1 (shPRDM1) or CREBBP (shCREBBP), and PRDM1 encoding fragments (oePRDM1) were inserted into adenovirus vectors, and the corresponding adenovirus particles were packaged in HEK-293A cells. After a 48-h infection, cells were harvested for further study. In addition, cells were treated with 4 μM SGC-CBP30 (Yuanye Bio-Technology Co., Ltd, cat# S81370 Shanghai, China), a highly specific CREBBP/EP300 antagonist.

Real-time PCR assay

Total RNA was extracted with the TRIpure solution (BioTeke, cat# RP1001, Beijing, China) from the collected placentas and cells. Total RNA was reverse-transcribed into first-strand cDNA, and real-time PCR was performed by using the SYBR PCR Master Mix (Solarbio, cat# SY1020, Beijing, China). The mRNA expression was determined via $2^{-\Delta Ct}$ and $2^{-\Delta\Delta Ct}$ methods and normalized to *β-actin*. The primers were designed as follows: homo PRDM1 F, 5′-GAACGCCAACAGGAAATA-3′, R, 5′-AAAGTCCCGACAATACCAC-3'; homo CREBBP F, 5′-GCATTGATAACAGAGTCCCTAA-3′, R, 5′-TCTCCGTCTTCATTTCCAG-3'; homo EP300 F, 5′-GGCTGTATCAGAGCGTATT-3′, R, 5′-TGCTGTCTCCCTTGGTC-3'; rat PRDM1 F, 5′-CGACCTTAGCGACAACG-3′, R, 5′-TGACCTTTACAGGCACCAG-3'; rat CREBBP F, 5′-ATCCTATGGACCTTTCTACC-3′, R, 5′-AGCCACGCATTGTTGA-3'; homo β-actin F, 5′-GGCACCCAGCACAATGAA-3′, R, 5′-TAGAAGCATTTGCGGTGG-3'; rat β-actin F, 5′-GGAGATTACTGCCCTGGCTCCTAGC-3′, R, 5′-GGCCGGACTCATCGTACTCCTGCTT-3'.

Western blot analysis

Total proteins obtained from EOPE and NP placental samples (n = 4/each group) as well as cell lysates were isolated using the lysis buffer containing PMSF, and the protein concentrations were determined by the Bicinchoninic acid kit (Beyotime, cat# P0012 Shanghai, China). Protein lysates were separated by SDS-PAGE gels and transferred to the PVDF membranes (Millipore, Billerica, USA). Membranes were blocked in 5% non-fat milk or 3% BSA (for phosphorylated antibodies) and were probed overnight at 4 °C with primary antibodies. To magnify the protein signals, corresponding secondary HRP-conjugated antibodies were used to incubate the membranes for 45 min. The immune complexes were developed with the enhanced chemiluminescent substrate. Band intensities were imaged using the ImageJ software. The primary antibodies including: PRDM1 (1:1000; Novus Biologicals, cat# NB600-235, China), CREBBP (1:500; Affinity, cat# AF0861, China), MMP2 (1:500; Proteintech, cat# 10373-2-AP, China), and MMP9 (1:1000; Proteintech, cat# 10375-2-AP, China). Secondary antibodies including: goat anti-rabbit (1:5000; Beyotime, cat# A0208, China) or goat anti-mouse (1:5000; Beyotime, cat# A0216, China).

Immunohistochemistry analysis

Samples from the chorionic plate and the placental bed were also collected for immunohistochemical analysis. The paraffin-embedded placental tissues from control and EOPE patients and L-NAME-treated rats were deparaffinized and hydrated. Following incubation with 3% hydrogen peroxide, the slides were blocked with 1% BSA after antigen recovery. The slides were incubated with PRDM1 antibody (1:200; Novus Biologicals, cat# NB600-235SS, Littleton, USA), human leukocyte antigen primary antibody (HLA-G, 1:200, Bioss, cat# bs-0752R, China), or CREBBP antibody (1:50; Affinity Biosciences, cat# AF0861 Cincinnati, USA) at 4°C overnight. Following primary antibody incubation, the sections were incubated with HRP-labeled secondary antibody for 1 h at 37°C. The specimens were counterstained with hematoxylin, and images were captured using a light microscope (Olympus, Tokyo, Japan) at ×200 and ×400 magnification.

Immunofluorescence staining

For double immunofluorescence staining, paraffin-embedded sections from placental tissues were deparaffinized and blocked with 1% bovine serum albumin. The samples were incubated at 4 °C overnight with PRDM1 antibodies (1:50, Novus Biologicals, cat# NB600-235SS, Littleton, USA) combined with CK7 primary antibody (1:100, Abcam, cat# ab181598, China) or HLA-G (1:100, Bioss, Bioss, cat# bs-0752R, China). The sections were then incubated with a mixture of secondary antibodies. The nuclei were counterstained with DAPI, and the staining was visualized by the fluorescence microscope (Olympus, Japan).

TUNEL assay

Cell apoptosis in placental tissues was detected by terminal deoxynucleotidyl transferase-mediated dUTP nick end-labeling (TUNEL) assay using the *In Situ* Cell Death Detection Kit (Roche Diagnostics, cat# 12156792910, Indianapolis, USA) according to the manufactory's protocols. Briefly, placental tissues were collected from rats and fixed with 4% paraformaldehyde, embedded in paraffin, and sliced into 5 μm-thick sections. The slices were permeabilized with 0.1% Triton X-100 (Beyotime, Shanghai, China) and incubated in the TUNEL reaction regent 37°C for 60 min in the dark. Samples were blocked in 1% BSA and incubated at 4°C overnight with primary antibody against CK7 (1:100, Abcam, China) and visualized with the secondary antibodies. The nucleus was counterstained with DAPI. TUNEL-positive cells (labeled with green fluorescence) and CK7-positive cells (labeled with red fluorescence) in tissues were captured under a fluorescence microscope.

Cell counting Kit-8 (CCK-8) and annexin V-FITC/PI analysis

The capacity of trophoblast cells was examined using a CCK-8 kit (KeyGen, cat# KGA317, Nanjing, China). In brief, ten microliters of CCK-8 were added. Two hours later, the absorbance value was measured at 450 nm using an enzyme-linked immunosorbent assay plate reader. Primary trophoblast cells and HTR-8/Svneo cells were harvested and subjected to flow cytometry detection by Annexin V-FITC Apoptosis Detection Kit (KeyGen, cat# KGA108 Nanjing, China) according to the manufacturer's instructions. For cell apoptosis analysis, cells were stained with Annexin V-FITC and propidium iodide for 5 min. The apoptotic cells were then analyzed using flow cytometer software (NovoCyte, Agilent, Santa Clara, USA).

Transwell assay

Cell invasion and migration assays were performed using Transwell chambers. The chambers were pre-coated with 40 μL Matrigel (for invasion assays; Corning Incorporated, Corning, cat# 356234, USA), followed by a 2-h incubation at 37°C for solidification. The cultured medium (700 μL) containing 10% FBS was added to the bottom compartments. HTR-8/SVneo cells or primary trophoblast cells (5×10^4 per well for invasion and 5×10^3 per well for migration) in 300 μL cultured medium were seeded in the upper Transwell chamber and incubated for 48 h. Non-migrated or invaded cells were removed from the upper chamber. Cells that penetrated the membrane were fixed with 4% paraformaldehyde for 20 min and stained with 0.5% crystal violet for 5 min. The invaded and migrated cells were captured at ×200 magnification (Olympus, Tokyo, Japan).

Luciferase reporter assay

HEK293 cells (5×10^4 per well) were seeded in a 96-well plate. CREBBP promoter (−2000∼+10) was inserted into the pGL3-basic plasmids upstream to the firefly luciferase between NheI and XhoI restriction enzyme sites (General Biosystems, Anhui, China). pRL-TK expressing Renilla luciferase was used as an internal control. PRDM1 encoding fragment was inserted into pcDNA3.1 plasmids (pcDNA3.1-PRDM1, YouBio Technology Co., Ltd, Changsha China). Both the pcDNA3.1-PRDM1, pGL3-basic plasmids, and pRL-TK plasmids were co-transfected with into HEK293 cells. After 48 h, the luciferase activity of each well was measured using a Dual-Luciferase Reporter Assay System (KeyGen, Nanjing, cat# KGAF040, China) and normalized with the Renilla luciferase.

Chromatin immunoprecipitation (ChIP)

ChIP assay was employed by using the ChIP Assay Kit (Beyotime, cat# P2078, Shanghai, China) following the manufacturer's manuals. Briefly, cells were treated with 1% formaldehyde for 10 min to cross-link proteins with DNA. Cells were incubated with SDS cell-lysis buffer for 10 min on ice. The samples were sonicated for three 10s pulses on ice to generate DNA fragments. Then, the DNA-protein complex was immunoprecipitated with an antibody against PRDM1 or IgG overnight. The DNA-protein complex was treated with Protein A/G agarose for 1 h. The DNA fragments were purified using the Immune Complex Wash Buffer. The genomic regions containing PRDM1 binding sites (shown in Figure 6) were amplified via real-time PCR.

Oligonucleotide pull-down assay

Oligonucleotide pull-down assay was performed as described previously.[62] In brief, oligonucleotides containing PRDM1 binding sites (−1992 to −1983 bp and −489 to −479 bp) on CREBBP promoter were biotinylated and incubated with streptavidin magnetic beads for 30 min. The biotinylated double-stranded oligonucleotides were incubated with DNA beads buffer. DNA-protein complex was immobilized with streptavidin-agarose beads. The proteins were subjected to Western blot analysis.

QUANTIFICATION AND STATISTICAL ANALYSIS

All data were displayed as means ± SD and the analysis was performed by the software GraphPad Prism version 8.0 (GraphPad Software Inc., San Diego, USA). The results are presented as mean ± SD values. Student's t test or one-way analysis of variance with Tukey's post-hoc analysis was used to analyze statistical significance. The results were deemed statistically significant at $p < 0.05$.